

ManuRAG: Multi-modal Retrieval Augmented Generation for Manufacturing Question Answering

Yunqing Li^{2†}, Zihan Dong^{3†}, Farhad Ameri^{1*}, Jianbang Zhang²

¹ School of Manufacturing Systems and Networks, Arizona State University, Mesa, AZ, 85212, USA .

² AI Technology Center, Lenovo, Morrisville, NC, 27560, USA .

³ Computer Science Department, Georgia Institute of Technology, Atlanta, GA, 30332, USA .

*Corresponding author(s). E-mail(s): Farhad.Ameri@asu.edu;
Contributing authors: yli59@lenovo.com; puma122707@gmail.com;
zhangjb2@lenovo.com;

†These authors contributed equally to this work.

Abstract

The evolution of digital manufacturing requires intelligent Question Answering (QA) systems that can seamlessly integrate and analyze complex multi-modal data, such as text, images, formulas, and tables. Conventional Retrieval Augmented Generation (RAG) methods often fall short in handling this complexity, resulting in subpar performance. We introduce ManuRAG, an innovative multi-modal RAG framework designed for manufacturing QA, incorporating specialized techniques to improve answer accuracy, reliability, and interpretability. To benchmark performance, we evaluate ManuRAG on three datasets comprising a total of 1,515 QA pairs, corresponding to mathematical, multiple-choice, and review-based questions in manufacturing principles and practices. Experimental results show that ManuRAG₄ consistently outperforms existing methods across all evaluated datasets. Furthermore, ManuRAG's adaptable design makes it applicable to other domains, including law, healthcare, and finance, positioning it as a versatile tool for domain-specific QA.

Keywords: Retrieval augmented generation, Multi-modality, Manufacturing question answering, Large language models

1 Introduction

1.1 Background and Motivation

As Industry 4.0 continues to evolve and expand, QA systems play a crucial role in leveraging big data in manufacturing. A QA system is a type of information retrieval system designed to automatically answer questions posed by users in natural language. These systems use a combination of natural language processing, machine learning, and often knowledge bases or large datasets to understand the question and generate an appropriate answer. By facilitating data-driven decision-making, QA systems provide engineers, operators, and managers with accurate and relevant insights across diverse data formats. This accessibility is important for intelligent manufacturing, where data from sensors, machines, and design files must be integrated seamlessly to enable efficient and accurate production. Integrating information retrieval with systems that prioritize connectivity, automation, and secure collaboration enables manufacturers to streamline the entire value creation process—from ideation and production to sustainment and adaptation. These advanced capabilities promote self-organizing, intelligent production systems and ensure reliable, secure communication across the manufacturing value chain. Additionally, QA systems are crucial for achieving interoperability, enabling seamless interaction between legacy and next-generation equipment and platforms, and for evaluating the impact of external factors across a product's entire life cycle. Potential users of manufacturing QA systems include mechanical design engineers calculating precise tolerances, production engineers optimizing assembly processes, machine operators implementing temperature adjustments, quality assurance teams verifying dimensional accuracy, and research teams exploring advanced materials and techniques for manufacturing efficiency.

1.2 Challenges

The complexity of manufacturing data presents a unique challenge for effective information retrieval and QA. Manufacturing documents span a wide array of data types, including text, images, formulas, Computer-aided design (CAD) models, tables, sensor data, and videos [1–3]. Each format holds critical information necessary for understanding and optimizing manufacturing processes, designs, and operational insights. For example, text data may contain operational guidelines, maintenance logs [4], or compliance records that require natural language processing for efficient retrieval. Images, like defect photos or assembly line snapshots, demand computer vision techniques to identify patterns or detect quality issues. Formulas and equations, embedded in documentation, need precise recognition and interpretation to enable accurate replication and troubleshooting of complex processes. Together, these varied data formats underscore the important role of advanced information extraction and processing techniques for efficient, data-driven manufacturing insights.

The adoption of Manufacturing QA systems in industry remains in its early stages, driven by the growing complexity of manufacturing processes and the increasing need for advanced data management solutions. GPT-powered chatbots [5], such as those offered by Streebo [6], represent some of the closest analogs. However, these tools

primarily focus on conversational interactions, lacking the robust multi-modal retrieval and domain-specific reasoning capabilities required for comprehensive Manufacturing QA applications.

Traditional information retrieval methods for Manufacturing QA are typically limited to either text-based or image-based data retrieval, often failing to capture the full context and complexities of multi-modal information. This limitation can lead to inefficiencies in production workflows and hinder effective decision-making. For instance, in design and development departments—especially within complex industries like automotive manufacturing—retrieving relevant information across various data formats presents considerable challenges. An engineer, for example, might need to answer a multiple-choice question identifying which vehicle model employs a five-link suspension system. The relevant evidence may be distributed across heterogeneous document types: legacy models may be documented primarily in textual specifications, more recent models may embed suspension details within PDF files containing technical drawings, and newer designs may rely on CAD models, exploded views, or annotated images. Manually sifting through these formats is time-intensive, increases the risk of missing key details, and becomes even more difficult with extensive documentation. This example highlights a core issue: the pressing need for a robust retrieval system that can seamlessly integrate and interpret text, visual data, and structured tables in a way that meets the complex needs of design and manufacturing.

Several factors limit today's information retrieval systems for QA tasks in the manufacturing domain. Manufacturing data is diverse, complex, and technical, requiring specialized processing for each type [7–9]. Textual data involves domain-specific terminology, while visual data like figures, tables, and slides demand advanced interpretation tools—capabilities lacking in many current systems. Another challenge is transforming text and image data into a unified format computers can process, with minimal information loss [10, 11]. These issues lead to misinterpretation or loss of critical details, hindering efficient data retrieval and integration. Advanced multi-modal retrieval approaches are crucial to enable faster, accurate decision-making in modern manufacturing.

1.3 Objectives

To overcome these limitations, we introduce a multi-modal RAG system tailored for Manufacturing QA. This system seamlessly integrates and processes various data types—such as images, formulas, tables, and text—to deliver a deeper and more contextually accurate understanding of manufacturing documents. By bridging the gap between diverse data formats and complex manufacturing queries, multi-modal RAG empowers users with actionable insights that are both reliable and comprehensive. It enables more informed decision-making, streamlines workflows, improves operational efficiency, and minimizes production errors, ultimately enhancing productivity and driving innovation in manufacturing systems.

This paper leverages multi-modal data integration and retrieval to enhance Manufacturing QA and decision support. The main contributions of this paper include:

1. Develops a complete multi-modal QA pipeline for the manufacturing domain, from extracting information in text, images, formulas, and tables to generating answers, to support product design, bottleneck identification, and data-driven decision-making.
2. Compares standalone large language models (LLMs), RAG-augmented LLMs, and multi-modal RAG-augmented LLMs, evaluating their strengths and limitations across different question types, including mathematical, multiple-choice, and review-based formats.
3. Introduces and compares indexing and retrieval strategies for multi-modal data, examining how pre- and post-embedding alignment of textual and visual content impacts QA accuracy and interpretability.

The remainder of the paper is organized as follows: in Section 2, we review related work. Section 3 introduces how we construct ManuRAG. In Section 4, we present experiments demonstrating the effectiveness of our approach. Finally, Section 5 discusses the limitations of our method and suggests directions for future work.

2 Related Work

2.1 Question Answering Systems

QA systems have evolved notably, leveraging a range of techniques to retrieve and respond to queries [12]. Traditional expert systems, built on domain-specific expertise, have long been used in QA tasks but often lack scalability and adaptability for complex, data-rich environments. Large language models (LLMs) such as Generative Pre-trained Transformer (GPT) [13] and Transformer-based models [14], including Bidirectional Encoder Representations from Transformers (BERT), have introduced major advancements in QA by using deep learning to interpret queries and retrieve relevant information from extensive datasets. These models excel in understanding context and language, making them effective in general-purpose QA. Multi-modal models have further advanced the field, enabling visual question answering by combining image and text processing [15] and supporting QA with the integration of tabular and textual data for contextually rich responses [16]. However, none of these models are suitable for the manufacturing domain due to the complexity and technical nature of manufacturing data. Manufacturing QA requires precise extraction and robust integration of diverse, multi-modal data types which presents a unique challenge beyond the capabilities of existing QA models.

2.2 Information Extraction

Information extraction has evolved to handle diverse formats in structured and unstructured data, including text, images, tables, and multimedia. Multimedia documents, such as PDFs, pose unique challenges because they integrate text, images, tables, and sometimes audio or video. Advanced data extraction approaches use layout detection models [17, 18] to identify content regions. Formula recognition relies on deep learning methods [19–21]. Optical Character Recognition (OCR) tools [22, 23] are essential for accurate text extraction across fonts and languages, providing detailed

information extraction capabilities for multimedia content. Data extraction in manufacturing involves extracting information from text, images, and other data types to support decision making. For text, Li et al. [24] developed methods to extract knowledge from manufacturer websites, streamlining service discovery. For images, Bhandarkar and Nagi [25] convert geometric data into higher-level manufacturing insights. Despite the prevalence of multimedia in manufacturing, few studies have focused on extracting information from these diverse sources, highlighting a research gap.

2.3 Prompt Engineering and Retrieval Augmented Generation

While LLMs excel at general QA, they struggle in manufacturing contexts because they often lack domain knowledge, cannot handle specialized terminology or interpret technical data (e.g., CAD files, sensor readings, process parameters), and may produce imprecise or hallucinated answers when fine-grained accuracy is required [26]. Manufacturing queries require precise, domain-specific knowledge that LLMs are prone to producing plausible but incorrect answers (hallucinations) [27], cannot reliably provide without specialized grounding, making them insufficient for manufacturing QA without further refinement.

Prompt engineering involves crafting prompts to guide LLMs toward accurate, contextually relevant responses. Techniques like Chain of Thought (CoT) [28] and Tree of Thought [29], enhance this process by promoting multi-step reasoning, enabling LLMs to handle complex queries more effectively. In manufacturing QA, prompt engineering integrates industry-specific language and technical constraints into tailored prompts, enabling LLMs to produce precise, domain-relevant answers and effectively manage specialized terminology and complexity [30, 31].

Another powerful approach is RAG, which grounds LLM outputs in external knowledge by retrieving relevant documents or databases from real-world manufacturing data. Tools like Llama-Index [32] and LangChain [33] enable efficient text-based retrieval, while GraphRAG [34] introduces graph-based retrieval for reasoning over interconnected data. RAG methods, such as text-embedding RAG and graph-embedding RAG, match queries with documents or capture relationships within complex, interconnected information sources. In manufacturing, RAG has been applied to retrieve domain-specific terms [35], integrate ontological knowledge graphs for engineering analysis, and support materials design [36]. Multi-modal RAG—an emerging extension that integrates text, images, and other data types to provide richer context for complex questions [37]—has shown promise in healthcare but has not yet been tailored for the manufacturing domain.

Multi-modal large language models (MLLMs) [38, 39] have substantially advanced the integration of text and visual data. While these MLLMs excel in understanding multi-modal inputs, they are constrained by input token limits, which pose challenges when processing massive amounts of information.

Multi-modal RAG overcomes this limitation by indexing both textual and visual content and fetching the most relevant context at inference time, thus enabling efficient access to extensive external knowledge sources. Whereas standard RAG operates

solely on text, multi-modal RAG fuses image and document embeddings, typically following one of two strategies: (1) converting images into descriptive text for seamless integration into text-based workflows, and (2) aligning text and image data in a shared embedding space using multi-modal embeddings like Contrastive Language-Image Pre-Training (CLIP) [40] and Jina-CLIP [41]. These methods enable models to retrieve and reason across modalities, enhancing their performance on tasks that require both visual and textual comprehension. While multi-modal RAG has shown applications in domains such as healthcare, its potential remains underexplored in manufacturing. The manufacturing domain demands tailored solutions capable of handling intricate schematics, technical diagrams, and process-specific content with high precision and contextual relevance.

3 Method

Traditional RAG systems are primarily designed to handle text inputs, often overlooking the multi-modal nature of information present in real-world data. To overcome this limitation, we propose ManuRAG, an extension of RAG that incorporates multi-modality to process diverse data types from manufacturing documents. The MLLM employed in ManuRAG accepts both plain text and images as inputs, enabling it to process *.pdf* files (PDFs) through a pipeline of object detection and text recognition models. This process effectively categorizes documents into distinct parts such as figures, images, formulas, and textual content.

The ManuRAG framework comprises four key stages: multi-modal data extraction, indexing, retrieval, and answer generation. A state-of-the-art PDF extraction pipeline—integrating advanced vision and segmentation models—helps robust figure and content recognition [42]. Details of the multi-modal data extraction process are presented in Section 3.1. Indexing mechanisms are discussed in Section 3.1.4, retrieval strategies in Section 3.3, and answer generation approaches in Section 3.4.

Additionally, we introduce four variations of the ManuRAG framework. These variations explore different strategies for integrating multi-modal data. The details of these variations are presented in Section 3.5.

3.1 Multi-modal Data Extraction

Using original manufacturing files directly in RAG presents notable challenges. These files often contain complex structures, including images, tables, formulas, and non-standard text layouts, which make direct use infeasible for efficient information retrieval. Converting PDFs to plain text frequently results in the loss of crucial contextual and structural information, yielding low-quality data that undermines the performance of manufacturing QA. To address these challenges, we focus on extracting and organizing multi-modal data—text, images, tables, and formulas—from manufacturing PDFs to create a robust input for RAG systems.

The primary goal of this section is to construct high-quality data representations that accurately capture fundamental manufacturing knowledge while minimizing noise. This process begins with extracting and processing information from manufacturing PDF files to create separate text and image representations, ensuring the

preservation of critical data. Using the pdf-extract-kit framework [42], we employed state-of-the-art methodologies for multi-modal data extraction. This includes layout detection to maintain the document’s structure, formula extraction to keep mathematical content, and image and table extraction to incorporate visual data. OCR was applied to digitize textual content from non-selectable regions. These multi-modal representations are then embedded and stored in a unified database that preserves relationships between different modalities, enabling seamless integration and effective use in downstream tasks.

3.1.1 Layout Detection

Accurate layout detection is crucial for maintaining the structural integrity of manufacturing PDFs and extracting relevant content effectively. This process entails parsing documents into distinct elements while filtering out irrelevant contents, such as page numbers or repeated headers, that could negatively impact QA performance. To this end, we adopt the trained LayoutLMv3 base model [18], which was pre-trained on 11 million pages from the IIT-CDIP [43] corpora using AdamW ($\beta_1 = 0.9$, $\beta_2 = 0.98$), a base learning rate of 1×10^{-4} with linear warmup, and a weight decay of 1×10^{-2} . To detect regions, we apply the pretrained LayoutLMv3 token-classification head to assign each token (or image patch) one of the layout labels (image, table, title, or text), using the highest-probability prediction for each region. By isolating these regions at the token level, our pipeline ensures that only semantically meaningful content is indexed and passed to the RAG framework.

3.1.2 Formula Extraction

Our formula extraction pipeline comprises two sequential stages. First, we employ a fine-tuned YOLOv8 [44] model with an input resolution of 1280 pixels, a confidence threshold of 0.25, and an intersection over union threshold of 0.45 to accurately locate both inline and display-style formulas. Second, each detected region is passed to the UniMERNNet model [45] to convert formula images directly into L^AT_EX source code. This unified detection-and-recognition approach—illustrated by examples such as $E = \frac{\sigma}{\epsilon}$ for Young’s modulus and $J = -D \frac{\partial C}{\partial x}$ for Fick’s first law—ensures spatial accuracy, minimizes recognition errors, and preserves the semantic fidelity of mathematical expressions.

3.1.3 Image and Table Extraction

Our table extraction pipeline follows a two-stage process. First, we detect and segment table regions using PaddleOCR [46], which identifies cell boundaries and overall table layout within page crops. Second, each segmented table image is processed by StructEqTable [47] to convert detected tables into clean L^AT_EX, HTML, or Markdown code. This streamlined approach preserves complex cell relationships, formatting, and numerical precision, enabling our QA system to leverage richly structured tabular data in downstream retrieval and reasoning.

3.1.4 Optical Character Recognition

After removing non-textual elements, the remaining page regions are processed by PadleOCR, which outputs Markdown-formatted text annotated with bounding-box and element-type metadata. Each extracted text segment and visual element is assigned a 128-bit Universally Unique Identifier (UUID), enabling consistent cross-referencing and seamless integration within our QA pipeline.

3.2 Indexing

Indexing plays a crucial role in RAG, as it helps efficient and accurate retrieval of relevant information during query resolution. In ManuRAG, indexing involves structuring and storing multi-modal data, including both textual and visual information, to enable seamless integration into subsequent retrieval and generation tasks. By projecting data into a high-dimensional embedding space, the system ensures compatibility with similarity-based searches, which are important for effective information retrieval.

3.2.1 Text Vector Database

Textual data, including paragraphs, formulas and links to the images, is pre-processed dividing it into manageable chunks to preserve contextual relevance and coherence. This segmentation process is governed by two key parameters: the chunk size, which defines the maximum length of each segment, and the chunk overlap, which determines the degree of overlap between consecutive chunks to maintain continuity of context. Given a textual input $Text$, the division into overlapping chunks can be expressed as:

$$\text{Chunks} = \{C_i : C_i = Text[i : i + S], i = 0, S - O, 2(S - O), \dots\} \quad (1)$$

where S represents the chunk size, O denotes the chunk overlap, C_i is the i -th chunk, and $|Text|$ is the total length of the text.

We model each chunk C_i as

$$C_i = (Text_i, Img_i), \quad Img_i = \{Img_{i1}, \dots, Img_{ib_i}\}. \quad (2)$$

Here, $Text_i$ is the full textual content of the i -th chunk, and Img_i is the set of all images referenced in that chunk (with Img_{ij} denoting the j -th image).

The chunks are projected into the embedding space using a LLM-based text embedding model Embed_{Text} . The embedding for each chunk C_i is represented as:

$$v_{C_i} = \text{Embed}_{Text}(C_i) \quad (3)$$

These embeddings, along with their corresponding text chunks, are stored in a text vector database, enabling efficient retrieval during the query resolution process.

3.2.2 Image Vector Database

For visual data—including extracted figures and tables—a multi-modal embedding model is employed to project all content into the same space as the text embeddings. This model handles both $Text$ and Img modalities, enabling cross-modal search (for

example, text-to-image and image-to-text retrieval). To align with CLIP’s native training resolution, each visual element Img_j is first resized so that its shorter side measures 224 pixels and then center-cropped to a 224×224 pixel square. It is then encoded into an embedding vector v_{Img_j} via the multi-modal embedding function Embed_{MM} :

$$v_{Img_j} = \text{Embed}_{\text{MM}}(Img_j) \quad (4)$$

The resulting image embeddings, along with their associated image data, are stored in an image vector database. This database is designed to support the retrieval of visual information and to complement the textual data during queries.

Although the multi-modal embedding model is capable of processing both text and images, its understanding of complex and lengthy textual content is not as good as that of most LLM-based text embedding models. The text embedding model, which is trained specifically on extensive textual datasets, provides a deeper understanding of intricate text structures and semantics. To capitalize on the strengths of both approaches, some variations of ManuRAG maintain separate vector databases for text and images. The details are explained in Section 3.5. This dual-database approach enables ManuRAG to effectively leverage the specialized capabilities of the text embedding model and the flexibility of the multi-modal embedding model.

3.3 Retrieval

Retrieval is a key part of RAG system, enabling the system to identify and extract the most relevant information from the indexed data. In ManuRAG, retrieval serves the critical function of narrowing down the multi-modal data—text and images—stored in vector databases, so that only the most pertinent chunks are provided as context to the language model for producing answers to manufacturing-related questions. By incorporating retrieval, the system ensures efficiency and accuracy in handling large and diverse datasets.

The retrieval process is based on calculating the similarity between the embedding of an input manufacturing query and the embeddings of stored data. The similarity metric used is cosine similarity, defined as:

$$\text{Sim}(q, v) = \frac{q \cdot v}{\|q\| \|v\|} \quad (5)$$

where q is the embedding of the input manufacturing question Q , and v is the embedding vector of each stored item (text chunk or image). Cosine similarity measures the angular similarity between the query embedding and stored embeddings, providing a reliable estimate of their relevance.

3.3.1 Retrieval from the Text Vector Database

For textual data, the system calculates cosine similarity between the query embedding and each indexed chunk embedding. Using Eq. 5, the top- K text chunks are retrieved as

$$\text{Top@K}_{text} = \arg \max_{\{C_i\}} \text{Sim}(q_1, v_{C_i}), \quad (6)$$

where q_1 is the query embedding in text space, and v_{C_i} is the embedding of chunk C_i . Once these K chunks C_{i_1}, \dots, C_{i_K} are selected, the set of all images they reference is

$$\bigcup_{r=1}^K Img_{i_r} = \bigcup_{r=1}^K \{ Img_{i_r1}, Img_{i_r2}, \dots \}. \quad (7)$$

3.3.2 Retrieval from the Image Vector Database

For visual data, the input query is encoded into the same embedding space as the image embeddings using a multi-modal embedding model. Cosine similarity is then calculated between the query embedding and the image embeddings stored in the image vector database. The top k images with the highest similarity scores are retrieved:

$$Top@K_{Img} = \arg \max_{\{Img_j\}} \text{topK}(\text{Sim}(q_2, v_{Img_j})). \quad (8)$$

Here, q_2 is the query embedding in the multi-modal space, and v_{Img_j} is the embedding of image Img_j , enabling direct retrieval of relevant visual data via embedding similarity.

3.4 Answer Generation

Answer generation is the final stage of the RAG pipeline, where the system synthesizes a response to the input query by leveraging the relevant data retrieved during the retrieval phase. This step involves integrating the retrieved textual and visual information with the manufacturing question and processing it through an LLM or MLLM to produce an accurate and contextually appropriate answer.

3.4.1 Answer Generation Using Text-Only Retrieval Data

In the first strategy, the system combines the retrieved textual data, the manufacturing question, and the domain-specific prompt as input to a large language model (LLM) optimized for text-based processing. This approach excludes any retrieved visual data, focusing solely on textual context for answer synthesis. The process can be expressed as

$$A_{LLM} = \text{LLM}(\text{concat}(P, Q, Top@K_{text})), \quad (9)$$

where P is the specially designed prompt for questions in the manufacturing domain, Q represents the input query. This strategy is efficient and suitable for cases where the retrieved textual data alone provides sufficient context to answer the query. However, it does not account for visual information, which may limit its effectiveness for multi-modal queries.

3.4.2 Answer Generation Using Multi-modal Retrieval Data

In the second strategy, the system combines the textual data, the visual data and the manufacturing question as input to an MLLM. This approach incorporates both

text and images, enabling the model to consider visual context alongside textual information for answer generation. The generated answer can be formulated as follows:

$$A_{MLLM} = MLLM(\text{concat}(P, Q, \text{Top}@K_{text}, \text{Top}@K_{Img}, \bigcup_{r=1}^K Img_{i_r})). \quad (10)$$

This strategy generates answers by using relevant images from two sources: the images referenced in the top- K text chunks, $\bigcup_{r=1}^K Img_{i_r}$, and the images retrieved directly from the image vector database, $\text{Top}@K_{Img}$. Note that either of these image sets may be empty if no visual data is linked, indexed, or successfully retrieved.

We include our designed prompts for different types of manufacturing questions in Appendix A, and further describe the differences among the ManuRAG variations in Section 3.5.

3.5 ManuRAG Variations

We propose four variations of the ManuRAG framework to investigate the optimal approach for aligning textual and visual data in manufacturing QA. Specifically, the framework explores different strategies for integrating text and image data—whether alignment should occur before embedding, within the embedding space, or after embedding. Figure 1 highlights the workflows of each variation, emphasizing the differences in multi-modal data handling, indexing strategies, and answer generation methods.

ManuRAG₁ processes both textual and visual data by embedding textual information into a text vector database and visual data into an image vector database. Answer generation is performed using an MLLM.

ManuRAG₃ extends ManuRAG₁ by prioritizing the retrieval of visual data linked within the retrieved text chunks. It uses both text and image vector databases for indexing but focuses on retrieving images referenced in the text.

ManuRAG₂ simplifies ManuRAG₃ by eliminating the image vector database. It operates exclusively on textual data, storing embeddings in a text vector database, and generates answers using a LLM.

ManuRAG₄ introduces a unique step in multi-modal data processing. After identifying visual data referenced in the text, the visual content (for example, figures and tables) is transformed into descriptive text using an MLLM. This transformed text is then indexed in the text vector database and the answers are generated using an LLM (or optionally an MLLM). This variation aligns textual and visual data before embedding by converting visual data into a text-based representation. However, this transformation may result in some information loss, especially when the original visual context is critical.

4 Experiments

In this section, we present experiments to evaluate the effectiveness of the proposed methods for Manufacturing QA using real-world datasets to ensure practical relevance. The study focuses on evaluating how different RAG systems improve the performance

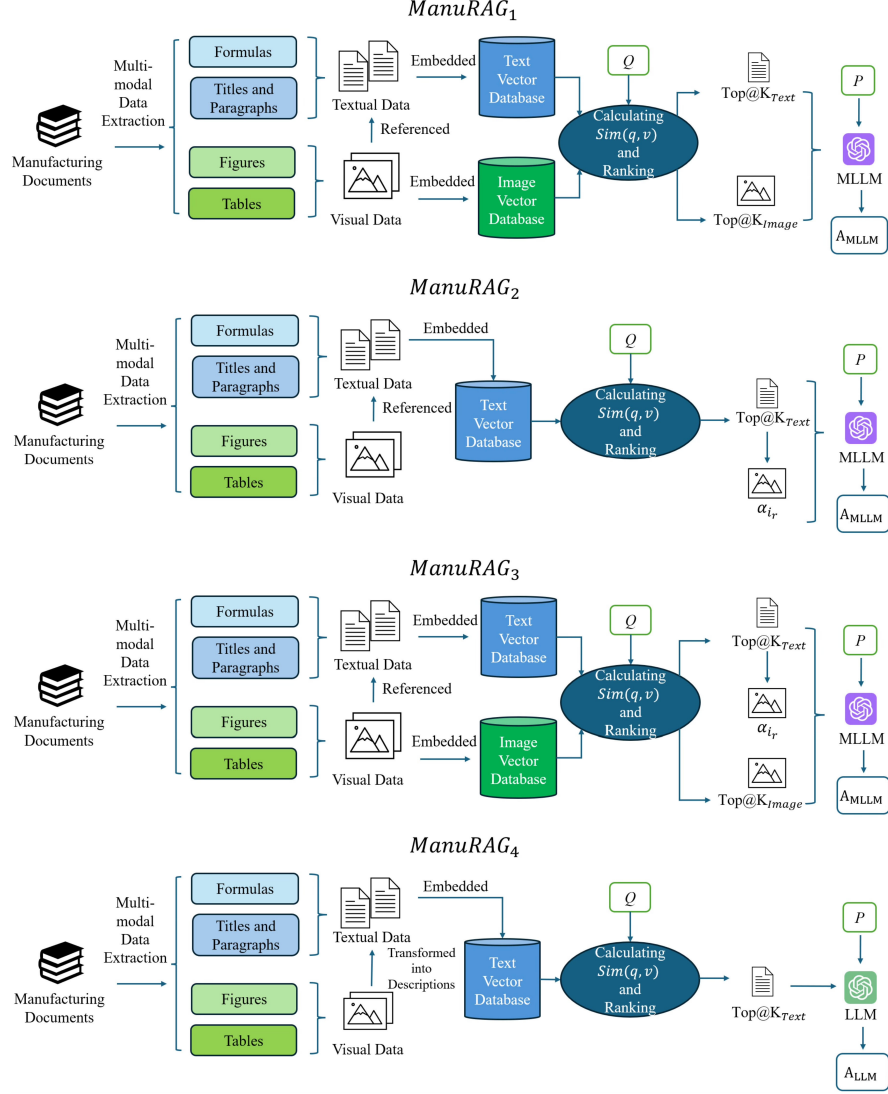


Fig. 1 Four Types of ManuRAG Frameworks

of Manufacturing QA and examining the influence of context precision and context recall on the effectiveness of these systems in retrieving relevant information. The experimental settings, including datasets, baselines, and configurations, are detailed in Section 4.1, while the evaluation metrics are introduced in Section 4.2. The general performance of the models and the context-retrieval-related performance are discussed in Sections 4.3 and 4.4.

4.1 Settings

4.1.1 Baselines and Configurations

We evaluate multiple variations of ManuRAG against alternative QA solutions to demonstrate the performance improvements and unique advantages offered by our approach. All models in the comparison leverage the same underlying MLLM, GPT-4O, ensuring a consistent foundation for multi-modal capabilities. Our evaluation encompasses the baseline GPT-4O, both in its standard configuration and with manufacturing-specific prompts, as well as various RAG models, including traditional and multi-modal RAG approaches.

All RAG models employ Ada v2 for text indexing and retrieval, CLIP for image indexing and retrieval when an image vector store is used, and GPT-4O for generating final answers. Both the ManuRAG variants and the RAG methods are built using the LlamaIndex framework [32]. The source documents for RAG context retrieval are derived from the same PDF version of a textbook, *Fundamentals of Modern Manufacturing* [48], which is a widely recognized textbook covering engineering materials, manufacturing processes, and electronics technologies.

All experiments are conducted in Google Colab with $k = 1$, $S = 600$, and $O = 100$, following Edge et al. [49] and Lewis et al. [50]. Except for the baseline models, all other models use a unified prompt configuration, as detailed in Appendix A. Below are additional details about the benchmark models:

- **GPT-4O:** Direct QA using GPT-4O without any specialized prompts.
- **GPT-4O (CoT):** Direct QA enhanced with Chain-of-Thought (CoT) prompting to enable step-by-step reasoning with GPT-4O.
- **RAG:** RAG applied to raw text directly extracted from the files, excluding any visual data.
- **RAG_{hq}:** A high-quality RAG framework utilizing structured text extracted using the method outlined in Section 3.1.
- **ManuRAG₁₋₃:** Variants of multi-modal RAG, as described in Section 3.5.
- **ManuRAG₄:** A variant of multi-modal RAG introduced in Section 3.5, incorporating GPT-4O to transform image data into text for enriched contextual understanding.

4.1.2 Evaluation Datasets

We evaluate our benchmarks using three datasets consisting of 1,515 question-answer pairs derived from the official solutions of *Fundamentals of Modern Manufacturing* [48]. Notably, this dataset is excluded from the content used for RAG retrieval. The datasets are organized as follows:

- **MathQ:** 309 mathematical QA pairs requiring factual accuracy and semantic understanding, often multi-modal with formulas, tables, and figures. Preprocessing excludes excessively long questions/answers (over 600 tokens) or trims sub-questions for LLM compatibility.

- **MCQ:** 471 multiple-choice questions (MCQs) evaluating the ability to select the correct option—some requiring multi-modal analysis. Answers are formatted as distinct choices (a–d) and include explanations to ensure precise evaluation.
- **RQ:** 735 review QA pairs focusing on comprehension and reasoning over textual content to evaluate conceptual understanding.

Examples of each type of datasets are provided in Appendix B.

4.2 Evaluation Metrics

We adopt five evaluation metrics from RAGAS [51] with GPT-4 to comprehensively evaluate the performance of QA models which are Factual Correctness, Semantic Similarity, Recall-Oriented Understudy for Gisting Evaluation (ROUGE), Context Precision and Context Recall. The metrics and their formulas are as follows.

4.2.1 Factual Correctness

Factual correctness measures the F1 score of answers by comparing them to the ground truth and is applied across all evaluated models. This metric evaluates the degree to which the response aligns with the reference, with scores ranging from zero to one, where higher values indicate better performance. GPT-4 is employed to decompose both the response and the reference into distinct claims, with natural language inference used to evaluate the factual overlap between them. By balancing precision and recall through the F1 score, this metric provides a comprehensive measure of the accuracy of the generated answers relative to the reference.

True Positive (TP) represents the number of claims in the answer that are present in the reference. False Positive (FP) indicates the number of claims in the response that are not present in the reference, while False Negative (FN) corresponds to the number of claims in the reference that are not present in the answer. Using these values, the precision, recall, and F1 score are calculated as follows:

$$\text{Precision} = \frac{\text{TP}}{\text{TP} + \text{FP}} \quad (1)$$

$$\text{Recall} = \frac{\text{TP}}{\text{TP} + \text{FN}} \quad (2)$$

$$\text{Factual Correctness (F1 Score)} = \frac{2 \times \text{Precision} \times \text{Recall}}{\text{Precision} + \text{Recall}} \quad (3)$$

4.2.2 Semantic Similarity

Semantic similarity evaluates how semantically close the generated answer is to the reference answer, which is applied across all evaluated models. It is measured using a cross-encoder model that computes a semantic similarity score ranging from zero to one. A higher score indicates a better semantic alignment between the generated answer and the ground truth.

4.2.3 Recall-Oriented Understudy for Gisting Evaluation

ROUGE measures the lexical overlap between generated answers and reference answers, and is used here to evaluate text-based responses for MCQs. It measures the overlap of n -grams ($n = 1$) using the F1 score to quantify similarity between the response and the reference. The formula for ROUGE is defined as follows:

$$\text{Precision}_n = \frac{\text{Number of overlapping } n\text{-grams}}{\text{Total number of } n\text{-grams in the generated answer}} \quad (11)$$

$$\text{Recall}_n = \frac{\text{Number of overlapping } n\text{-grams}}{\text{Total number of } n\text{-grams in the reference}} \quad (12)$$

$$\text{ROUGE}_n = \frac{2 \times \text{Precision}_n \times \text{Recall}_n}{\text{Precision}_n + \text{Recall}_n} \quad (13)$$

This metric provides a straightforward and effective way to test lexical similarity in MCQ dataset, where exact matches of words or phrases are crucial for evaluation.

4.2.4 Context Precision

Context precision measures the relevance of retrieved context chunks to the query. It evaluates the proportion of relevant chunks among the retrieved contexts in RAG-based models, including RAG₁, RAG₂, and ManuRAG₁ to ManuRAG₄. This metric incorporates a weighted precision approach, where v_k represents the weight assigned to each chunk at rank k . The precision at rank k ($top_k = 3$) is computed as:

$$\text{Precision}@k = \frac{\text{TP}@k}{\text{TP}@k + \text{FP}@k} \quad (1)$$

Using these precision values, the context precision for the top K results is calculated as:

$$\text{Context Precision}@K = \frac{\sum_{k=1}^K (\text{Precision}@k \times v_k)}{\text{Total number of relevant items in Top}@K} \quad (2)$$

4.2.5 Context Recall

Context recall measures the percentage of relevant context retrieved compared to the total relevant context available among the retrieved contexts in RAG-based models. Ground Truth (GT) refers to the set of reference claims or facts that are correct and are used as a standard for evaluation. This metric calculates how many of the claims in the ground truth are attributable to the retrieved contexts. The formula for context recall is given as:

$$\text{Context Recall} = \frac{|\text{GT attributed to retrieved contexts}|}{|\text{Total number of claims in GT}|} \quad (1)$$

Table 1 Comparison of Different Metrics Across Methods for Manufacturing QA (Highest performance for each dataset is highlighted in **bold**). We compare six benchmark models; the method that integrates images and text before indexing (ManuRAG₄) outperform those that treat modalities separately, achieving the optimal factual-correctness scores across all tasks.

Category	Factual Correctness (%)	Semantic Similarity (%)
MathQ		
GPT-4O	49.91	87.03
GPT-4O(CoT)	56.22	86.85
RAG	59.51	87.66
RAG _{hq}	59.48	87.90
ManuRAG ₁	19.14	77.03
ManuRAG ₂	56.69	87.32
ManuRAG ₃	55.31	87.32
ManuRAG ₄	62.03	87.82
MCQ		
GPT-4O	6.99	77.60
GPT-4O(CoT)	78.58	94.79
RAG	85.22	96.52
RAG _{hq}	86.38	96.62
ManuRAG ₁	86.82	95.27
ManuRAG ₂	60.54	91.20
ManuRAG ₃	61.62	90.15
ManuRAG ₄	87.61	96.82
RQ		
GPT-4O	38.01	89.93
GPT-4O(CoT)	40.47	89.92
RAG	45.51	91.08
RAG _{hq}	45.64	91.12
ManuRAG ₁	45.34	90.97
ManuRAG ₂	40.53	91.15
ManuRAG ₃	39.10	91.13
ManuRAG ₄	45.75	91.00

4.3 Overall Performance

The performance of Manufacturing QA models, shown in [Table 1](#), demonstrates that ManuRAG₄ consistently achieves the best performance across all three datasets. It achieves the highest factual correctness in MathQ, outperforming GPT-4O and GPT-4O with CoT, indicating its strength in handling mathematical reasoning. For MCQ tasks, it also scores highest in factual correctness and ROUGE ([Table 2](#)). In RQ tasks, while the differences across models are smaller due to the simpler, text-based nature of the questions, ManuRAG₄ still achieves the highest factual correctness, confirming its overall effectiveness.

ManuRAG₄’s broader superiority can be attributed to two key mechanisms. First, its position-aware, unified indexing converts each image into descriptive text and embeds it at its original location alongside surrounding paragraphs, thereby preserving the natural document flow; this co-location of visual descriptions and adjacent text is particularly well suited to domain-rich documents (for instance, textbooks or technical papers) and enables more effective matching during retrieval. Second, by removing the separate image index, ManuRAG₄ minimizes the retrieval of irrelevant diagrams or icons—reducing “visual noise” and sharpening both context precision and factual correctness. Together, these advantages allow ManuRAG₄ to strike a more effective balance between relevance and coverage than variants that either maintain independent image stores or forgo positional integration of visual content.

While ManuRAG₄ consistently delivers the highest results, other configurations, such as ManuRAG₁ and ManuRAG₂, show strengths in specific tasks. For example, ManuRAG₁ performs well on MCQ and RQ tasks by effectively leveraging image retrieval through links embedded in the textual context but performs poorly on MathQ, indicating limitations in its ability to handle mathematical reasoning with this retrieval method. The low performance of ManuRAG₃ suggests that retrieving more images does not necessarily lead to better answers for Manufacturing QA. We include QA example comparisons across different models in Appendix B.

Across all datasets, the inclusion of CoT reasoning improves GPT-4O’s performance, showcasing its effectiveness in enhancing logical reasoning and precision for QA tasks. RAG_{hq} demonstrates better performance than RAG, highlighting the effectiveness of the multi-modal data extraction method.

Semantic similarity scores are generally high across all models and datasets, reflecting alignment with reference answers. However, semantic similarity alone does not guarantee factual correctness, particularly in MathQ and MCQ, where precise reasoning and retrieval are critical. While semantic similarity remains useful for assessing general alignment, factual correctness is a more reliable indicator of performance in Manufacturing QA tasks.

4.4 Context-based Performance

While factual correctness evaluates the alignment of generated answers with GT, it does not evaluate the quality of retrieved context, which is critical in RAG-based models. Context precision and recall provide additional insights by measuring the relevance and coverage of the retrieved context, offering a deeper understanding of how well the model supports its generated answers. This section evaluates both the quality of the generated answers and the completeness of the retrieved context, as shown in Table 3.

By aligning text and image data before embedding, ManuRAG₄ achieves superior integration and strong performance across tasks. It demonstrates robust performance across datasets, achieving the highest context precision for MathQ and MCQ, high recall for MCQ and RQ, and effectively balancing relevance and coverage for retrieval-augmented tasks. RAG_{hq} excels in context precision for RQ, emphasizing the importance of high-quality indexed textual data, while standard RAG, with shorter indexed text, achieves the highest recall for MathQ and competitive recall for MCQ

Table 2 ROUGE Scores for MCQs Across Different Models. The highest scores are achieved by ManuRAG₄, and RAG_{hq}, suggesting that joint text–image embedding or high-quality text indexing is associated with more faithful multiple-choice answer generation.

Model	ROUGE (%)
GPT-4O	10.35
GPT-4O(CoT)	77.61
RAG	86.10
RAG _{hq}	86.71
ManuRAG ₁	81.19
ManuRAG ₂	63.13
ManuRAG ₃	58.88
ManuRAG ₄	86.77

and RQ, highlighting a trade-off between precision and recall. In contrast, ManuRAG₁, ManuRAG₂, and ManuRAG₃ show competitive precision for RQ but struggle with MathQ precision and lower recall for MathQ and MCQ, reflecting the limitations of separate vector stores for text and image data.

Across our evaluated benchmarks, ManuRAG₄ and RAG_{hq} consistently rank among the top performers in context precision and factual correctness. Although converting images into text inevitably results in some loss of visual information, ManuRAG₄ nevertheless surpasses the other variants across different manufacturing question types. This observation indicates that—even when certain visual cues (for example, precise axis labels or schematic annotations) are simplified—the joint integration of textual and visual content prior to retrieval is more effective than maintaining separate image indices. When images are indexed independently, they lose their contextual linkage with the surrounding text; in manufacturing documents, many images and accompanying paragraphs often convey critical information only when considered together. Furthermore, independent retrieval of images can introduce “visual noise” in the form of irrelevant diagrams or icons, which may undermine the benefits of preserving complete visual data.

5 Conclusion and Future Work

Advances in digital manufacturing demand intelligent QA systems capable of integrating and analyzing complex multi-modal data. Traditional RAG methods often struggle to process such data effectively. ManuRAG tackles these challenges by presenting the multi-modal RAG framework, specifically designed for Manufacturing QA. Experimental results demonstrate that ManuRAG₄ outperforms existing methods, offering valuable insights into selecting appropriate RAG strategies and aligning image and text data for diverse manufacturing scenarios. Beyond manufacturing, ManuRAG’s

Table 3 Context Recall and Precision for MathQ, MCQ, and RQ. Methods that integrate text and image embeddings prior to retrieval are associated with higher context precision and recall, demonstrating the benefit of preserving co-located semantics; text-only retrieval also performs strongly when high-quality textual context is available.

Category	Context Precision (%)			Context Recall (%)		
	MCQ	MathQ	RQ	MCQ	MathQ	RQ
RAG	81.95	92.56	92.24	33.39	67.83	81.23
RAG _{hq}	85.35	93.20	93.74	34.61	57.00	81.27
ManuRAG ₁	79.41	33.66	92.79	33.36	30.95	81.47
ManuRAG ₂	80.89	33.33	92.52	32.01	22.98	80.63
ManuRAG ₃	79.41	33.33	92.65	33.44	20.47	80.86
ManuRAG ₄	86.84	93.53	91.84	37.88	62.26	81.56

adaptable design positions it as a versatile tool for domain-specific QA in areas such as law, healthcare, and finance.

Experimental results show that effective context alignment between textual and visual data improves manufacturing QA performance. In contexts such as textbooks, images and accompanying text often share semantic content; aligning these modalities before embedding preserves their co-location and produces more coherent and relevant representations. Simply increasing the number of retrieved images does not guarantee better performance; retrieval strategies should prioritize the relevance and integration quality of images. For mathematical reasoning, robust multi-modal alignment significantly enhances performance. For tasks heavily reliant on text, simpler retrieval methods can achieve competitive results if high-quality textual contexts are well-indexed.

However, even ManuRAG₄, the top-performing configuration, still falls short of perfect accuracy, particularly on queries that require precise interpretation of technical drawings and process schematics—showing that domain-specific QA remains an open challenge and highlighting the usefulness of our benchmark in exposing these gaps. These limitations point to three improvement paths: fine-tune, adapt, or replace existing multi-modal encoders—such as Jina-CLIP [41] on manufacturing-specific corpora to enhance visual-text alignment and achieve more accurate, domain-tailored image or text retrieval; integrate advanced retrieval designs from recent RAG frameworks [52, 53] to balance precision and recall; and extend the system to support richer data types and document formats—such as CAD models [54], instructional videos [55], enterprise work orders, maintenance manuals, and time-series sensor logs—by developing specialized embedding strategies [56] to ensure robustness across diverse manufacturing information sources.

Appendix A Prompt Design

The following shows the prompt designed for MathQ:

MathQ Prompt

As a manufacturing expert, solve the math question step by step using the provided context and your knowledge of manufacturing calculations. Make sure to clearly explain your reasoning:

{context_str}

Question:

Query: {query_str}

Answer:

The following presents the prompt designed for MCQ:

MCQ Prompt

As a manufacturing expert, answer the following multi-choice questions based on the provided context step by step. Select the correct letter choices only.

Answer format:

“Explanation”: “Your explanation here.”, “YourChoice”: “Answer. (d), (e), and (g).”

{context_str}

Answer the following question:

Query: {query_str}

Answer:

The following shows the prompt designed for RQ:

RQ Prompt

You are an expert in manufacturing major. You need to answer the following short response question based on the context and your knowledge of manufacturing processes and materials. Please provide a detailed explanation and justify your answer. Be concise, clear, and accurate.

{context_str}

Answer the following question:

Query: {query_str}

Answer:

Appendix B QA Examples

This section presents QA examples of different types and their answers generated by three different models, specifically comparing GPT-4O (CoT), traditional RAG, and the best-performing ManuRAG variant.

B.1 MathQ Example

The following is an example of QA pairs from MathQ. ManuRAG₄ generates correct answers, whereas RAG and GPT-4O (CoT) fail. GPT-4O (CoT) cannot reference Table 4.1 or the associated formulas from the manufacturing documents, limiting its accuracy. While RAG retrieves relevant formulas from the text data, it is constrained by its inability to access visual information, such as the data in Table 4.1 (from the textbook).

MathQ Problem

The starting diameter(D) of a shaft is 25.00 mm. This shaft is to be inserted into a hole in an expansion fit assembly operation. To be readily inserted, the shaft must be reduced in diameter by cooling. Determine the temperature to which the shaft must be reduced from room temperature(T) 20°C to reduce its diameter to 24.98 mm. Refer to Table 4.1.

Correct Answer

For steel, $\alpha = 12 \times 10^{-6}$ mm/mm/°C according to Table 4.1. Revise Eq. (4.1) to:

$$D_2 - D_1 = \alpha D_1 (T_2 - T_1)$$

Substitute the known values:

$$24.98 - 25.00 = 12 \times 10^{-6} \cdot 25.00 \cdot (T_2 - 20)$$

Simplify:

$$-0.02 = 300 \times 10^{-6} \cdot (T_2 - 20)$$

$$-0.02 = 0.0003(T_2 - 20)$$

$$-0.02 = 0.0003T_2 - 0.006$$

$$-0.02 + 0.006 = 0.0003T_2$$

$$-0.014 = 0.0003T_2$$

$$T_2 = \frac{-0.014}{0.0003}$$

$$T_2 = \underline{-46.67^\circ\text{C}}$$

GPT-4O (CoT)

To solve this problem, we need...

Calculation: Step 1: Understand the Concept of Thermal Contraction...

Step 4: Use the Provided Table to Find the Coefficient of Linear Expansion...

Since specific data (Table 4.1) is mentioned but not provided here, let's assume...

Step 6: Calculate the Final Temperature...

Using the assumed coefficient of linear expansion, the calculated temperature is:

$$T_2 = -52.73^\circ\text{C}$$

Conclusion: The shaft must be cooled to approximately -52.73°C to achieve the desired diameter reduction from 25.00 mm to 24.98 mm.

RAG

To solve this problem, we need...

Calculation The formula for the change in diameter due to thermal expansion or contraction is given by:

$$D_2 - D_1 = \alpha \cdot D_1 \cdot (T_2 - T_1)$$

First, calculate the change in diameter... Using the coefficient of linear thermal expansion (α), the temperature is calculated as:

$$T_2 = -48.39^\circ\text{C}$$

Conclusion: The shaft must be cooled to approximately -48.39°C to achieve the desired diameter reduction for the expansion fit assembly operation.

ManuRAG₄

To solve this problem, we need...

The change in diameter due to thermal contraction is given by:

$$D_2 - D_1 = \alpha \cdot D_1 \cdot (T_2 - T_1)$$

Calculation: 1. Calculate the change in diameter: ... 2. Substitute the values into the formula: ... 3. Calculate the temperature change:

$$T_2 = \frac{-0.02}{0.0003} + 20$$

$$T_2 = -46.67^{\circ}\text{C}$$

Conclusion: The shaft must be cooled to approximately -46.67°C to reduce its diameter from 25.00 mm to 24.98 mm for the expansion fit assembly operation.

B.2 MCQ Example

This question represents a MCQ problem for the manufacturing materials. GPT-4O (CoT) fails to generate a completely correct answer, whereas both RAG and ManuRAG₄ provide accurate responses. RAG and ManuRAG₄ achieves the correct result by effectively utilizing retrieved textual context from the manufacturing textbook.

MCQ Problem

Which of the following materials are used as fibers in fiber-reinforced plastics (FRPs) (select more than one): (a) aluminum oxide, (b) boron, (c) carbon/graphite, (d) epoxy, (e) Kevlar 49, (f) S-glass, and (g) unsaturated polyester.

Correct Answer

The correct materials used as fibers in FRPs are: (a), (b), (c), (e), and (f).

GPT-4O (CoT)

Explanation: Fiber-reinforced plastics (FRPs) are composite materials made of a polymer matrix reinforced with fibers to enhance their mechanical properties. In the given options: - (a) Aluminum oxide is typically not used as a fiber in FRPs; rather, it's more common as a ceramic or in powder form for reinforcement. - (b) Boron is indeed used as a fiber in certain high-performance FRPs. - (c) Carbon/graphite is one of the most common and effective fiber reinforcements. - (d) Epoxy is generally a type of polymer matrix in FRPs, not a fiber. - (e) Kevlar 49 is an aramid fiber known for high strength and is used in FRPs. - (f) S-glass is a specialized type of glass fiber used in FRPs for higher strength. - (g) Unsaturated polyester is also a type of polymer matrix and not used as a fiber.

Your Choice: (b), (c), (e), and (f).

RAG

Explanation: Fiber-reinforced plastics (FRPs) are composite materials that consist of a polymer matrix reinforced with fibers. According to the provided context, the principal fiber materials used in FRPs include glass (such as E-glass and S-glass), carbon, and Kevlar 49. Additionally, less common fibers mentioned are boron, silicon carbide (SiC), aluminum oxide, and steel. Epoxy and unsaturated polyester are not fibers; they are types of polymer matrices used in FRPs.

Your Choice: (a), (b), (c), (e), and (f).

ManuRAG₄

Explanation: The question asks for materials used as fibers in fiber-reinforced plastics (FRPs). Based on the provided context, the materials used as fibers in FRPs include: - (a) Aluminum oxide (Al_2O_3) is mentioned as a less common fiber material in FRPs. - (b) Boron is mentioned as a fiber used in advanced composites. - (c) Carbon/graphite is a principal fiber material in FRPs. - (e) Kevlar 49 is listed as a principal fiber material in FRPs. - (f) S-glass is a type of glass fiber used in FRPs.

Epoxy and unsaturated polyester are not fibers; they are matrix materials used in FRPs.

Your Choice: (a), (b), (c), (e), and (f).

B.3 RQ Example

The following is an example of review question in the dataset. GPT-4O (CoT) provides a comprehensive list but includes less relevant variables such as pressure and barriers, leading to less focus. RAG identifies the key variables accurately, leveraging retrieved

context but lacks consistency in prioritizing variables. ManuRAG₄ achieves the most concise and correct explanation by effectively retrieving and integrating context from relevant sources.

RQ Problem

What are the important variables that affect mass diffusion?

Correct Answer

According to Fick's first law, mass diffusion depends on the following variables:

- **Diffusion Coefficient:** The diffusion coefficient rises rapidly with temperature, so temperature is an important variable.
- **Concentration Gradient (dc/dx):** The difference in concentration of diffusing species across a distance.
- **Contact Area (A):** The area through which diffusion occurs.
- **Time:** The duration of the diffusion process.

GPT-4O (CoT)

Explanation: Mass diffusion is a critical process in manufacturing and materials science. The variables that affect diffusion include:

1. **Temperature:** Temperature is perhaps the most influential factor affecting diffusion. Higher temperatures increase atomic motion, accelerating diffusion.
2. **Concentration Gradient:** The concentration gradient, or the difference in concentration of diffusing species between two points, directly affects diffusion rates.
3. **Diffusing Species:** The size, mass, and chemical nature of the particles being diffused influence diffusion rates.
4. **Medium or Matrix Structure:** The structure of the material through which diffusion occurs is critical.
5. **Pressure:** In gases and, to some extent, in liquids, pressure can influence diffusion rates.
6. **Time:** Over longer periods, the extent of diffusion naturally increases as particles spread through the medium.
7. **Presence of Barriers or Interfaces:** Physical barriers or interfaces, such as coatings or phase boundaries, can alter the pathway and rate of diffusion.

RAG

Explanation: Mass diffusion in solids, particularly metals, is influenced by several key variables:

1. **Temperature:** A critical factor affecting diffusion, as higher temperatures increase atomic mobility.
2. **Concentration Gradient (dc/dx):** Represents the difference in concentration of diffusing species across a distance.
3. **Diffusion Coefficient:** A material-specific parameter that quantifies how easily atoms can move through a material.
4. **Crystal Structure and Defects:** Vacancies and other imperfections in the crystal structure facilitate atomic motion.
5. **Material Properties:** Atomic size, bonding, and lattice structure influence diffusion behavior.
6. **Surface Area (A):** The area of the boundary through which diffusion occurs.

ManuRAG₄

Explanation: The important variables that affect mass diffusion include:

1. **Temperature:** A critical factor in diffusion. Higher temperatures increase thermal agitation, allowing atoms to move more freely.
2. **Concentration Gradient (dc/dx):** The driving force for diffusion, representing the difference in concentration of atoms across a distance.
3. **Diffusion Coefficient :** A material-specific parameter that quantifies the ease with which atoms can move through a material.
4. **Time:** The duration over which diffusion occurs affects the extent of diffusion.
5. **Area of the Boundary (A):** The area through which diffusion occurs impacts the rate of mass transfer.

References

- [1] Tao, F., Qi, Q., Liu, A., Kusiak, A.: Data-driven smart manufacturing. *Journal of Manufacturing Systems* **48**, 157–169 (2018)
- [2] Letaief, M.B., Tlija, M., Louhichi, B.: An approach of cad/cam data reuse for manufacturing cost estimation. *International Journal of Computer Integrated Manufacturing* **33**(12), 1208–1226 (2020)
- [3] He, C., Liu, M., Zhang, Y., Wang, Z., Hsiang, S.M., Chen, G., Li, W., Dai, G.: Space–time–workforce visualization and conditional capacity synthesis in uncertainty. *Journal of Management in Engineering* **39**(2), 04022071 (2023)

- [4] Karray, M.H., Ameri, F., Hodkiewicz, M., Louge, T.: Romain: Towards a bfo compliant reference ontology for industrial maintenance. *Applied Ontology* **14**(2), 155–177 (2019)
- [5] OpenAI: ChatGPT (AutoCAD Master). <https://openai.com/chatgpt>. AI-powered assistant for AutoCAD and design-related guidance. Accessed January 26, 2025. (2025)
- [6] Streebo: ChatGPT in Manufacturing: Use Cases. <https://www.streebo.com/chatgpt-manufacturing-use-cases>. Accessed: 2025-01-26
- [7] Starly, B., Koprov, P., Bharadwaj, A., Batchelder, T., Breitenbach, B.: “unreal” factories: Next generation of digital twins of machines and factories in the industrial metaverse. *Manufacturing Letters* **37**, 50–52 (2023) <https://doi.org/10.1016/j.mfglet.2023.07.021>
- [8] Li, Y., Liu, X., Starly, B.: Manufacturing service capability prediction with graph neural networks. *Journal of Manufacturing Systems* **74**, 291–301 (2024)
- [9] Bharadwaj, A.G., Starly, B.: Knowledge graph construction for product designs from large cad model repositories. *Advanced Engineering Informatics* **53**, 101680 (2022)
- [10] Moro, G., Salvatori, S., Frisoni, G.: Efficient text-image semantic search: A multi-modal vision-language approach for fashion retrieval. *Neurocomputing* **538**, 126196 (2023) <https://doi.org/10.1016/j.neucom.2023.03.057>
- [11] Li, Y., Tang, Z., Zhuang, J., Yang, Z., Ameri, F., Zhang, J.: C-mag: Cascade multimodal attributed graphs for supply chain link prediction. *arXiv preprint arXiv:2508.08071* (2025)
- [12] Soares, M.A.C., Parreiras, F.S.: A literature review on question answering techniques, paradigms and systems. *Journal of King Saud University-Computer and Information Sciences* **32**(6), 635–646 (2020)
- [13] Liu, X., Zheng, Y., Du, Z., Ding, M., Qian, Y., Yang, Z., Tang, J.: Gpt understands, too. *AI Open* **5**, 208–215 (2024)
- [14] Vaswani, A.: Attention is all you need. *Advances in Neural Information Processing Systems* (2017)
- [15] Singh, A., Natarajan, V., Shah, M., Jiang, Y., Chen, X., Batra, D., Parikh, D., Rohrbach, M.: Towards vqa models that can read. In: *Proceedings of the IEEE/CVF Conference on Computer Vision and Pattern Recognition*, pp. 8317–8326 (2019)
- [16] Zhang, Z., Li, X., Gao, Y., Lou, J.-G.: Crt-qa: A dataset of complex reasoning

question answering over tabular data. In: Proceedings of the 2023 Conference on Empirical Methods in Natural Language Processing, pp. 2131–2153 (2023)

[17] Soto, C., Yoo, S.: Visual detection with context for document layout analysis. In: Proceedings of the 2019 Conference on Empirical Methods in Natural Language Processing and the 9th International Joint Conference on Natural Language Processing (EMNLP-IJCNLP), pp. 3464–3470 (2019)

[18] Huang, Y., Lv, T., Cui, L., Lu, Y., Wei, F.: Layoutlmv3: Pre-training for document ai with unified text and image masking. In: Proceedings of the 30th ACM International Conference on Multimedia, pp. 4083–4091 (2022)

[19] Gao, L., Yi, X., Liao, Y., Jiang, Z., Yan, Z., Tang, Z.: A deep learning-based formula detection method for pdf documents. In: 2017 14th IAPR International Conference on Document Analysis and Recognition (ICDAR), vol. 1, pp. 553–558 (2017). IEEE

[20] Zhou, M., Cai, M., Li, G., Li, M.: An end-to-end formula recognition method integrated attention mechanism. *Mathematics* **11**(1), 177 (2022)

[21] Terven, J., Córdova-Esparza, D.-M., Romero-González, J.-A.: A comprehensive review of yolo architectures in computer vision: From yolov1 to yolov8 and yolo-nas. *Machine Learning and Knowledge Extraction* **5**(4), 1680–1716 (2023)

[22] Ma, Y., Yu, D., Wu, T., Wang, H.: Paddlepaddle: An open-source deep learning platform from industrial practice. *Frontiers of Data and Domputing* **1**(1), 105–115 (2019)

[23] Thorat, C., Bhat, A., Sawant, P., Bartakke, I., Shirasath, S.: A detailed review on text extraction using optical character recognition. *ICT Analysis and Applications*, 719–728 (2022)

[24] Li, Y., Starly, B.: Building a knowledge graph to enrich chatgpt responses in manufacturing service discovery. *Journal of Industrial Information Integration* **40**, 100612 (2024)

[25] Bhandarkar, M.P., Nagi, R.: Step-based feature extraction from step geometry for agile manufacturing. *Computers in industry* **41**(1), 3–24 (2000)

[26] Xue, Z., Li, L., Tian, S., Chen, X., Li, P., Chen, L., Jiang, T., Zhang, M.: Domain knowledge is all you need: A field deployment of llm-powered test case generation in fintech domain. In: Proceedings of the 2024 IEEE/ACM 46th International Conference on Software Engineering: Companion Proceedings, pp. 314–315 (2024)

[27] Martino, A., Iannelli, M., Truong, C.: Knowledge injection to counter large language model (llm) hallucination. In: European Semantic Web Conference, pp.

182–185 (2023). Springer

- [28] Wei, J., Wang, X., Schuurmans, D., Bosma, M., Xia, F., Chi, E., Le, Q.V., Zhou, D., *et al.*: Chain-of-thought prompting elicits reasoning in large language models. *Advances in neural information processing systems* **35**, 24824–24837 (2022)
- [29] Yao, S., Yu, D., Zhao, J., Shafran, I., Griffiths, T., Cao, Y., Narasimhan, K.: Tree of thoughts: Deliberate problem solving with large language models. *Advances in Neural Information Processing Systems* **36** (2024)
- [30] Xia, L., Li, C., Zhang, C., Liu, S., Zheng, P.: Leveraging error-assisted fine-tuning large language models for manufacturing excellence. *Robotics and Computer-Integrated Manufacturing* **88**, 102728 (2024)
- [31] Valentine, R., *et al.*: Prompt engineering on the engineering design process. In: DS 131: Proceedings of the International Conference on Engineering and Product Design Education (E&PDE 2024), pp. 449–454 (2024)
- [32] Contributors, L.: LlamaIndex: Interface between LLMs and external data sources. Accessed: 2024-10-09 (2024). <https://www.llamaindex.ai/>
- [33] Contributors, L.: LangChain: Building applications with large language models. Accessed: 2024-10-09 (2024). <https://www.langchain.com/>
- [34] Contributors, G.: GraphRAG: Graph-based Retrieval-Augmented Generation Framework. Accessed: 2024-10-09 (2024). <https://www.github.com/facebookresearch/graphrag>
- [35] Bei, Y., Fang, Z., Mao, S., Yu, S., Jiang, Y., Tong, Y., Cai, W.: Manufacturing domain qa with integrated term enhanced rag. In: 2024 International Joint Conference on Neural Networks (IJCNN), pp. 1–8 (2024). IEEE
- [36] Buehler, M.J.: Generative retrieval-augmented ontologic graph and multiagent strategies for interpretive large language model-based materials design. *ACS Engineering Au* **4**(2), 241–277 (2024)
- [37] Sun, T., Somalwar, A., Chan, H.: Multimodal retrieval augmented generation evaluation benchmark. In: 2024 IEEE 99th Vehicular Technology Conference (VTC2024-Spring), pp. 1–5 (2024). IEEE
- [38] Alayrac, J.-B., Donahue, J., Luc, P., Miech, A., Barr, I., Hasson, Y., Lenc, K., Mensch, A., Millican, K., Reynolds, M., *et al.*: Flamingo: a visual language model for few-shot learning. *Advances in neural information processing systems* **35**, 23716–23736 (2022)
- [39] Li, J., Li, D., Savarese, S., Hoi, S.: Blip-2: Bootstrapping language-image pre-training with frozen image encoders and large language models. In: International

Conference on Machine Learning, pp. 19730–19742 (2023). PMLR

[40] Radford, A., Kim, J.W., Hallacy, C., Ramesh, A., Goh, G., Agarwal, S., Sastry, G., Askell, A., Mishkin, P., Clark, J., *et al.*: Learning transferable visual models from natural language supervision. In: International Conference on Machine Learning, pp. 8748–8763 (2021). PMLR

[41] Xiao, H., Mastrapas, G., Wang, B.: Jina clip: Your clip model is also your text retriever. In: Multi-modal Foundation Model Meets Embodied AI Workshop@ ICML2024 (2024)

[42] OpenDataLab: PDF-Extract-Kit: A Comprehensive Toolkit for High-Quality PDF Content Extraction. <https://github.com/opendatalab/PDF-Extract-Kit> (2024)

[43] Lewis, D., Agam, G., Argamon, S., Frieder, O., Grossman, D., Heard, J.: Building a test collection for complex document information processing. In: Proceedings of the 29th Annual International ACM SIGIR Conference on Research and Development in Information Retrieval, pp. 665–666 (2006)

[44] Hussain, M.: Yolo-v1 to yolo-v8, the rise of yolo and its complementary nature toward digital manufacturing and industrial defect detection. *Machines* **11**(7), 677 (2023)

[45] Zhang, W., Li, F., Chen, Y., Sun, X., Zhou, M.: UniMERNet: A Unified Detection-and-Recognition Network for Mathematical Expressions. <https://github.com/opendatalab/UniMERNet>. Accessed: 2025-06-11 (2024)

[46] Authors, P.: PaddleOCR, Awesome multilingual OCR toolkits based on PaddlePaddle. <https://github.com/PaddlePaddle/PaddleOCR> (2020)

[47] Innovator, A.: StructEqTable-Deploy: High-Fidelity Table Recognition Toolkit. <https://github.com/Alpha-Innovator/StructEqTable-Deploy>. Accessed: 2025-06-11 (2023)

[48] Groover, M.P.: Fundamentals of Modern Manufacturing: Materials, Processes, and Systems. John Wiley & Sons, Hoboken, NJ, USA (2010)

[49] Edge, D., Trinh, H., Cheng, N., Bradley, J., Chao, A., Mody, A., Truitt, S., Metropolitansky, D., Ness, R.O., Larson, J.: From local to global: A graph rag approach to query-focused summarization. arXiv preprint arXiv:2404.16130 (2024)

[50] Lewis, P., Perez, E., Piktus, A., Petroni, F., Karpukhin, V., Goyal, N., Küttler, H., Lewis, M., Yih, W.-t., Rocktäschel, T., *et al.*: Retrieval-augmented generation for knowledge-intensive nlp tasks. *Advances in neural information processing systems* **33**, 9459–9474 (2020)

- [51] Es, S., James, J., Espinosa Anke, L., Schockaert, S.: RAGAs: Automated evaluation of retrieval augmented generation. In: Aletras, N., De Clercq, O. (eds.) Proceedings of the 18th Conference of the European Chapter of the Association for Computational Linguistics: System Demonstrations, pp. 150–158. Association for Computational Linguistics, St. Julians, Malta (2024). <https://aclanthology.org/2024.eacl-demo.16/>
- [52] Li, Y., Ko, H., Ameri, F.: Integrating graph retrieval-augmented generation with large language models for supplier discovery. *Journal of Computing and Information Science in Engineering* **25**(2), 021010 (2025) <https://doi.org/10.1115/1.4067389> https://asmedigitalcollection.asme.org/computingengineering/article-pdf/25/2/021010/7422522/jcise_25_2.021010.pdf
- [53] Sharma, K., Kumar, P., Li, Y.: Og-rag: Ontology-grounded retrieval-augmented generation for large language models. In: Proceedings of the 2025 Conference on Empirical Methods in Natural Language Processing, pp. 32950–32969 (2025)
- [54] Wu, S., Khasahmadi, A., Katz, M., Jayaraman, P.K., Pu, Y., Willis, K., Liu, B.: Cad-llm: Large language model for cad generation. In: Proceedings of the Neural Information Processing Systems Conference. neurIPS (2023)
- [55] Huang, B., Wang, X., Chen, H., Song, Z., Zhu, W.: Vtimellm: Empower llm to grasp video moments. In: Proceedings of the IEEE/CVF Conference on Computer Vision and Pattern Recognition, pp. 14271–14280 (2024)
- [56] Yue, Z., Wang, Y., Duan, J., Yang, T., Huang, C., Tong, Y., Xu, B.: Ts2vec: Towards universal representation of time series. In: Proceedings of the AAAI Conference on Artificial Intelligence, vol. 36, pp. 8980–8987 (2022)